Athens Journal of Sciences- Volume 5, Issue 3 – Pages 207-222

Ignition Source Effect on Modelling Hydrogen Premixed Combustion

By Mohamed A. Yehia[*]
Salah S. Ibrahim[†]
Mosaad Fawzy[‡]

This paper presents numerical study of premixed combustion of hydrogen-air mixtures inside a laboratory scale combustion chamber. The study is carried out on a premixed lean mixture of hydrogen/air flames with an equivalence ratio of 0.7. The main focus of the current work is to examine the effects of the way the source of ignition would have on the overall characteristics of combustion. An in-house Large Eddy Simulation (LES) modelling technique has been used to carry out the numerical simulations. The model predictions have been validated against available published experimental data where ignition has been introduced through the use of a laser beam. Successful numerical representation of the experimental initial and boundary conditions has resulted in good agreement between the experimental and numerical results for the generated combustion flame and pressure-time history. It was concluded that the combustion characteristics are sensitive to the size of the ignition source in terms of the timing occurrence of the peak pressure but not its magnitude. This finding has practical importance in analyzing explosion hazards, internal combustion engines and gas turbine combustors.

Keywords: *Ignition Source, Large Eddy Simulations, Turbulent Premixed Combustion.*

Introduction

Hydrogen has the potential to solve two major energy challenges that confront design engineers of practical combustion systems today: reducing dependence on petroleum imports and reducing pollution and greenhouse gas emissions. To accelerate the use of Hydrogen, its combustion characteristics need to be well understood. It is an aim of this paper to investigate the effects of the source of ignition on the characteristics of the flame resulting from the combustion of a lean mixture of hydrogen in air.

The high rates of generated pressure due to flame acceleration may be augmented by the turbulence generated through the presence of one or more obstacles in the form of equipment or buildings in the path of the flame propagation following ignition. Such phenomenon has attracted the interest of research for some time. Scientifically, such application lies within a complex reacting flow that has been traditionally simulated through computational fluid dynamics (CFD)

[*]Associate Professor & Head of Combustion Group, Department of Mechanical Power, Faculty of Engineering, Cairo University, Egypt.
[†]Department of Aeronautical and Automotive Engineering, Loughborough University, UK.
[‡]Research Assistant, Department of Mechanical Engineering, British University of Egypt, Egypt.

https://doi.org/10.30958/ajs.5-3-1 doi=10.30958/ajs.5-3-1

techniques. The solution of Reynolds Averaged Navier Stokes equations (RANS) though adequate for a wide variety of applications in the combustion field does not possess the minimum requirements for providing a validation with experimentally obtained data to a satisfying level. This is mainly due to the fact that modelling of turbulence assumes 'isotropic' distribution of turbulence, an assumption that is quite crude for the simulation of premixed turbulent combustion with a wrinkled flame-let sheet that is both sensitive to chemical kinetics and turbulence eddies and with length scales much shorter than the computational grid resolution leading to inability to capture the most interesting mechanisms of premixed combustion.

The incorporation of Large Eddy Simulation (LES) techniques was considered two decades ago a formidable challenge due to modelling complexities as well as heavy computational costs. The development and wide availability of computational abilities that made powerful machines within the hands of industry encouraged the combustion community to incorporate their CFD tools with sophisticated models that employ both LES with a sub-grid scale model (SGS). Several commercial user-friendly codes with enhanced pre- and post-processors to define the problem and provide the CFD in its alternative meaning (Colored Fluid Dynamics) with much less attention devoted to the implication of the multidisciplinary nature of the phenomena involved in the problem under consideration. This study, however, was executed employing PUFFIN, an academic progressing tool that has been developed by Sydney and Loughborough Universities, (Kirkpatrick et al., 2003) which is continuously developing versions reflecting the works of generations of researchers, (Gubba et al., 2007; Gubba, 2009; Malalasekera et al., 2013).

In LES, as the reaction zone thickness of the premixed flame to be resolved is thin, with a characteristic length scale much smaller than a typical LES filter width, an appropriate SGS model is vital to account for the SGS chemical reactions. Several modelling approaches such as flame surface density (Bray, 1990; Pope, 1988), flame tracking technique (G-equation) (Williams, 1985; Menon and Kerstein, 1992), artificially thickened flame (Veynante and Poinsot, 1997) and probability density function (PDF) (Moller et al., 1996) are successfully adapted from classical RANS to LES. Recently, (Duwig and Fuchs, 2007) have numerically modelled turbulent premixed flames by using a S^+ marker field. They developed a new equation for marker field to capture the laminar or turbulent flame propagation via a reactive diffusive balance equation. Further details are available in Ibrahim et al., (2009).

The Combustion Chamber

The combustion chamber used here was originally developed at the University of Sydney (Kent et al., 2005). It has a volume of 0.625 L with a square cross-section of 50 mm and a length of 250 mm as shown in Figure 1. Experimental data for the flame structure and generated overpressure have been published in Kent et al., (2005) and are used here for model validation. The combustion

chamber consists of three exchangeable solid baffle plates to allow for different configurations as shown in Figure 1. This chamber is of particular interest because of its smaller volume and potential to hold a flame propagating in strong turbulence.

The solid baffle plates used are of 50 x 50 mm aluminum frames constructed from a 3 mm thick sheet. This consists of five 4 mm wide bars each with a 5 mm wide space separating them, rendering a blockage ratio of 40%. The baffle plates are aligned at 90 degrees to the solid obstacle in the configuration employed in the present study. These baffle plates are named as B1, B2 and are located at 20 and 80 mm respectively from the ignition point. The combustion chamber has a built-in solid square obstacle of 12 mm in cross-section, which is centrally located at 96 mm from the ignition point running throughout the chamber cross-section, which causes significant formation to the flow turbulent eddies. The pressure is measured using Piezo-resistive pressure transducers with a range of 0-1 bar and a response time of 0.1 ms. The transducer utilizes quartz crystals to develop a charge relative to the pressure applied. The pressure transducer is positioned at the ignition end of the combustion chamber. The exact location is on the central plane of x-axis, 37 and 5 mm on y and z axis respectively from the left bottom of the chamber.

The introduction of baffle plates and the obstacle into the flow inside the chamber serve to increase the turbulence level and the flame propagation speed.

Figure 1. (a) *Cross Section of the Combustion Chamber* (b) *Dimensions of the Baffle Plates* (All Dimensions are in mm)

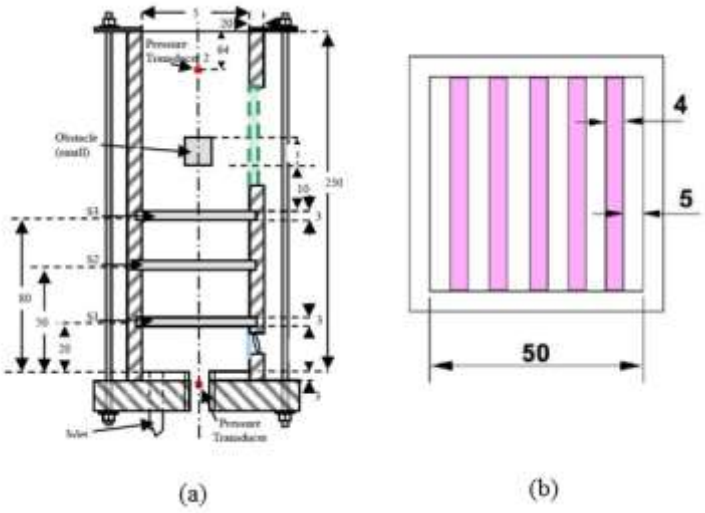

The Mathematical Model

Numerical results presented in this work are obtained using an LES code originally developed by Kirkpatrick (2002) and Kirkpatrick et al., (2003). The code solves the governing equations of the fluid flow, namely, conservation of mass, momentum, and energy. These equations are coupled with a transport equation for a reaction progress variable. The reaction progress variable c is

defined to vary from zero to one for the unburned fresh gases and the fully burned products, respectively. To be able to use LES, Favre filter is applied to the governing equations resulting in some unclosed terms which are modeled. Brief details of the filtered equations are given below.

In LES, the flow field is spatially filtered; a flow variable $\varphi(x,y,z,t)$ is decomposed of resolved component, $\bar{\varphi}(x,y,z,t)$ and unresolved component, $\grave{\varphi}(x,y,z,t)$. Scales are separated using a filter function G, and can be mathematically represented by convolution product as:

$$\bar{\varphi}(x,y,z,t) = \int_v G(x-x',y-y',z-z')\varphi(x,y,z,t)dx'dy'dz' \qquad (1)$$

The filter function G is associated with the cut-off length Δ, which is taken between Kolomogrov and integral length scales. The most commonly used filter functions are the cut-off filter, Gaussian filter, and box filter. The box or top hat filter is preferred in LES modeling of engineering applications due to its simplicity, it is expressed as:

$$G(x-x') = \begin{cases} \frac{1}{\bar{\Delta}} & if\ |x-x'| \le \frac{\bar{\Delta}}{2} \\ 0 & otherwise \end{cases} \qquad (2)$$

In the present work, the top-hat filter is used and the filtered governing equations in finite volume format are written by the application of box filter width of:

$$\Delta = (\Delta x \Delta y \Delta z)^{1/3} \qquad (3)$$

Where Δx, Δy, and Δz are the dimensions of the computational cell. The Favre filtered (mass weighted) transport equations of mass, momentum, energy and reaction progress variable are respectively given by:

The Favre-filtered continuity equation:

$$\frac{\partial \bar{\rho}}{\partial t} + \frac{\partial(\bar{\rho}\widetilde{u_j})}{\partial x_j} = 0 \qquad (4)$$

The Favre-filtered Navier-Stokes equation:

$$\frac{\partial \bar{\rho}\widetilde{u_i}}{\partial t} + \frac{\partial(\bar{\rho}\widetilde{u_i}\widetilde{u_j})}{\partial x_j} = -\frac{\partial \bar{P}}{\partial x_i} + \frac{\partial}{\partial x_j}\left(2\bar{\mu}\left[\tilde{S}_{ij} - \frac{1}{3}\delta_{ij}\tilde{S}_{kk}\right]\right) - \frac{\partial \tau_{ij}^{sgs}}{\partial x_j} \qquad (5)$$

Where $\tilde{S}_{ij}$ is the stress rate tensor and it is defined as:

$$\widetilde{S_{ij}} = \frac{1}{2}\left(\frac{\partial \widetilde{u_i}}{\partial x_j} + \frac{\partial \widetilde{u_j}}{\partial x_i}\right) \qquad (6)$$

τ_{ij}^{sgs} is the residual stresses which represent the effect of the unresolved (Sub-Grid-Scale, SGS) velocity components on the resolved ones. This term appears mathematically as a result of the non-linearity of the convection term in the Navier-Stokes equations. In the present work the residual stresses are modeled using the Smagorinsky model based on linear eddy viscosity and it is expressed as:

$$\tau_{ij}^{sgs} - \frac{1}{3}\delta_{ij}\tau_{ij}^{sgs} = -\bar{\mu}_{SGS}(\tilde{S}_{ij} - \frac{1}{3}\delta_{ij}\tilde{S}_{kk}) \quad (7)$$

The SGS eddy viscosity $\bar{\mu}_{SGS}$ can be expressed as a function of the filter size and the strain rate as:

$$\bar{\mu}_{SGS} = \bar{\rho}C_s\bar{\Delta}^2|\tilde{S}| \quad (8)$$

where $|\tilde{S}| = \sqrt{2\tilde{S}_{ij}\tilde{S}_{ij}}$ and C_s is the Smagorinsky model coefficient which is calculated by the dynamic procedure of Moin et al., (1991).

The Favre-filtered energy equation is written as:

$$\frac{\partial\bar{\rho}\tilde{h}}{\partial t} + \frac{\partial(\bar{\rho}u''_j h'')}{\partial x_j} = \frac{\partial\bar{P}}{\partial t} + 2\bar{\mu}\left[\tilde{S}_{ij} - \frac{1}{3}\delta_{ij}\tilde{S}_{kk}\right]:\frac{\partial\widetilde{u_j}}{\partial x_i} + \frac{\partial}{\partial x_j}\left(\frac{\bar{\mu}}{Pr}\frac{\partial\tilde{h}}{\partial x_j}\right) + \bar{\dot{q}}_c \quad (9)$$

The Favre-filtered reaction progress variable equation is given as:

$$\frac{\partial\bar{\rho}\check{c}}{\partial t} + \frac{\partial(\bar{\rho}\widetilde{u_j}\check{c})}{\partial x_i} + \frac{\partial(\overline{\rho u_j''c''})}{\partial x_j} = \frac{\partial}{\partial x_j}\left(\frac{\bar{\mu}}{Sc}\frac{\partial\check{c}}{\partial x_j}\right) + \overline{\dot{\omega}_c} \quad (10)$$

Scalar fluxes in equations (8) and (9) are modeled using a simple gradient transport model as:

$$\bar{\rho}u''_j h'' = \frac{\bar{\mu}_{SGS}}{Pr_t}\frac{\partial\tilde{h}}{\partial x_j} \quad (11)$$

$$\overline{\rho u_j''c''} = \frac{\bar{\mu}_{SGS}}{Sc_t}\frac{\partial\check{c}}{\partial x_j} \quad (12)$$

where Pr_t is the turbulent flow Prandtl number, Sc_t is the turbulent flow Schmidt number, and $\bar{\mu}_{SGS}$ is the sub-grid scale eddy viscosity.

The rate of the mean chemical reaction is modeled using the laminar flame-let approach (Poinot and Veynante, 2005), expressed as a function of the flame surface density and the mixture laminar burning velocity. The dynamics flame surface density (DFSD) approach is used to calculate the sub-grid scale chemical reaction rate. Brief details of the model are presented in this section. More details can be found in Gubba (2009).

The basis of the Flame Surface Density (FSD) model can be derived from the laminar flame-let approach. In this approach, the reaction zone is viewed as a group of thin, wrinkled, propagating layers. These layers, at high Damköhler number, are assumed to propagate at laminar flame speed. Hence, these propagating layers are considered as laminar flame-lets. The flame surface density, which describes the flame surface wrinkling by turbulence, is the flame surface area per unit volume, Σ. The mean chemical reaction rate can be written as a function of the FSD as:

$$\overline{\dot{\omega}_c} = R\bar{\Sigma} = \rho_u u_l \bar{\Sigma} \qquad (13)$$

Where ρ_u is the density of unburned mixture, $u_l$is the laminar burning velocity, and $\bar{\Sigma}$ is the flame surface density (FSD).

The mean filtered flame surface density is split into resolved and unresolved terms:

$$\bar{\Sigma} = |\overline{\nabla c}| = \prod(\bar{c}, \bar{\Delta}) + f(\bar{c}, \Delta, \prod(\bar{c}, \bar{\Delta})) \qquad (14)$$

The unresolved term can be evaluated using the following formulation:

$$\lambda = \bar{\Sigma} - \prod(\bar{c}, \bar{\Delta}) = |\overline{\nabla c}| - \prod(\bar{c}, \bar{\Delta}) \quad (15)$$

In this model the sub-grid scale contributions of unresolved flame surface density at test filter are assumed to be similar to that at the grid filter and related to each other using Germano identity (Germano et al., 1991). Test filter is applied to equation (14). Hence the mean filtered flame surface density can be written as:

$$\hat{\bar{\Sigma}} = |\widehat{\overline{\nabla c}}| = \prod\left(\hat{\bar{c}}, \hat{\bar{\Delta}}\right) + \left[|\widehat{\overline{\nabla c}}| - \prod\left(\hat{\bar{c}}, \hat{\bar{\Delta}}\right)\right] \qquad (16)$$

The second term in the above equation is the unresolved flame surface density at the test filter, which can be expressed as:

$$\Lambda = \left[|\widehat{\overline{\nabla c}}| - \prod\left(\hat{\bar{c}}, \hat{\bar{\Delta}}\right)\right] \qquad (17)$$

Therefore the unresolved contributions at test and grid filters are related to as follows:

$$\Lambda - \hat{\lambda} = \left[\prod(\widehat{\bar{c}, \bar{\Delta}}) - \prod\left(\hat{\bar{c}}, \hat{\bar{\Delta}}\right)\right] \qquad (18)$$

The sub-grid scale flame surface density contribution in the above equation can be added to the resolved term in equation (16) with a model coefficient, C_s. Hence the flame surface density is written as:

$$\bar{\Sigma} = \prod(\bar{c}, \bar{\Delta}) + C_s \left[\prod(\widetilde{\bar{c}, \bar{\Delta}}) - \prod\left(\hat{\bar{c}}, \hat{\bar{\Delta}}\right)\right] \qquad (19)$$

Using equations (17), (18) the unresolved terms in the above equations can be expressed as:

$$\prod(\widetilde{\bar{c}, \bar{\Delta}}) = \hat{\bar{\Sigma}}\left(\frac{\bar{\Delta}}{\delta_c}\right)^{D-2} \qquad (20)$$

$$\prod\left(\hat{\bar{c}}, \hat{\bar{\Delta}}\right) = \hat{\bar{\Sigma}}\left(\frac{\hat{\bar{\Delta}}}{\delta_c}\right)^{D-2} \qquad (21)$$

The model coefficient is dynamically obtained by identifying the sub-grid scale flame surface as a fractal surface, (Knikker et al., 2004). The two equations above are combined and γ is defined as the ratio between the test filter and the grid filter ($\hat{\bar{\Delta}}/\bar{\Delta}$), such that the test filter is greater than the grid filter.

$$C_s = \frac{1}{1-\gamma^{2-D}}\left[\left(\frac{\bar{\Delta}}{\delta_c}\right)^{D-2} - 1\right] \qquad (22)$$

The fractal dimension, D can be calculated using empirical equations, (North and Santavicca, 1990; Fureby, 2005) or can be dynamically calculated. In the present work, the fractal dimension D is dynamically calculated from:

$$D = 2.0 + \frac{\log\left(\left[\prod(\widetilde{\bar{c}, \bar{\Delta}})\right]/\left[\prod\left(\hat{\bar{c}}, \hat{\bar{\Delta}}\right)\right]\right)}{\log(\hat{\bar{\Delta}}/\bar{\Delta})} \qquad (23)$$

The Numerical Simulations

The LES model used here solves strongly coupled Favre filtered flow equations outlined above, which are written in a boundary fitted coordinates and discretized by using a finite volume method. The spatial discretization is done with finite volume method on a non-uniform staggered Cartesian grid. Second-order central difference is used for discretization of diffusion, advection, and pressure gradient terms in the momentum equation, while the third order QUICK scheme is used in the regions outside the chamber where the accuracy is less important. Second order central difference is also used for the pressure correction equation and diffusion terms in the scalar equations, whereas SHARP technique is used for advection terms. The fractional step method is used to advance all the equations in time.

The equations are advanced in time using the fractional step method. Crank Nicolson scheme is used for the time integration of momentum and scalar equations. A number of iterations are required at every time step owing to strong coupling of equations with one other. Solid boundary conditions are applied at the

bottom, vertical walls, for baffles and obstacle, with the power-law wall function used to calculate wall shear. Outflow boundary conditions are applied at the vented end of chamber. A non-reflecting boundary condition similar to commonly used convective boundary condition, in incompressible LES is used to avoid reflection of pressure waves at this boundary. The initial conditions are quiescent with zero velocity and reaction progress variable. Ignition is modelled by setting the reaction progress variable to 0.5 within a definite radius at the bottom center of the chamber.

The equations are solved using a Bi-Conjugate Gradient solver with an MSI pre-conditioner for the momentum, scalar and pressure correction equations. The time step is limited to ensure the CFL number remains less than 0.5 with the extra condition that the upper limit for δt is 0.3 ms. The solution for each time step requires around 8 iterations to converge, with residuals for the momentum equations less than 2.5e-5 and scalar equations less than 2.0e-3. The mass conservation error is less than 5.0e-8. Simulations were carried using a three dimensional, non-uniform, Cartesian co-ordinate system for compressible flow with low Mach number. Since this type of flow involves large changes in density, high velocities and significant dilatation, all terms in the governing equations are retained.

The Computational Domain

In order to simulate the turbulent premixed flame of the hydrogen/air mixture, a computational domain with initial and boundary conditions is required. The domain must extend in the direction normal to the outflow boundary to avoid any possible pressure reflections. However, to avoid certain numerical instabilities, in general, the domain is extended outside the combustion chamber.

A typical computational domain, superimposed with the numerical combustion chamber and obstacles is shown for clarity in Figure 2. The combustion chamber has dimensions of 50 x 50 x 250 mm. The flame propagates over the turbulence generating baffles and solid obstacle surrounded by solid wall boundary conditions. To ensure that the pressure wave leaves the chamber smoothly, without reflections, the open end of the domain is extended to 250 mm in the z-direction with a far-field boundary condition. Similarly, the domain is extended to 325 mm in the x and y directions with large expansion ratios approximately equal to 1.25 outside the combustion chamber. The numerical model has been employed with a computational grid of 90×90×336 (2.7 million) cells in 3 dimensional space (Figures 3, 4). It should be noted that any further grid refinement beyond this grid has no significant impact on the results (Gubba et al., 2007; Abdel-Raheem et al., 2013).

Figure 2. *The Computational Domain of the Combustion Chamber*

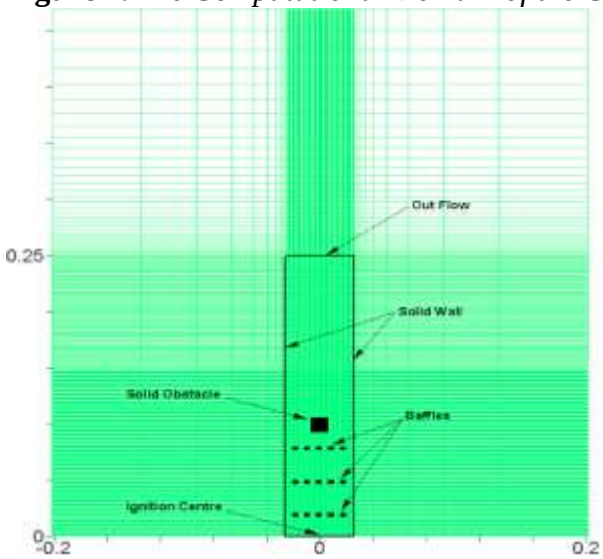

The Study Test Case

The test case studied in this work, shown in Figure 3, has two baffle plates and a small square solid obstacle of 12 mm in cross section. The plates and the obstacle are rendering a blockage ratio of 40% and 24% respectively.

The first baffle plate is located at a distance of 20 mm from the ignition source. As it is relatively close to the ignition point and the flame speed is slow, the effect of this obstacle on generating turbulence is small and this is why re-laminarization of the flame front is observed. The main objective of this baffle-plate is to accelerate the flame propagation and accordingly, achieve a peak pressure in shorter time.

The second baffle plate is located at a distance of 80 mm from the ignition end and it is the most effective plate in increasing turbulence level inside the combustion chamber. After hitting this baffle plate, the flame acceleration is maximum, thus turbulence level and flame speed are increased.

The square cross-sectional solid obstacle is located at a distance of 96 mm from the ignition end. Its purpose is not to increase the turbulence induced but rather to increase the blockage ratio and accordingly the flame front development. The flame fast acceleration is recorded after this obstacle and after which the flame is wrapped into the recirculation area and the distortion and mixing are enhanced at the flame front.

The other parameters used in the present work are equivalence ratio of 0.7, a lower heating value of 286,000 (kJ/kmol) and laminar burning velocity equals to 1.3 (m/s).

Figure 3. *Schematic Diagram of the Flow Configuration*

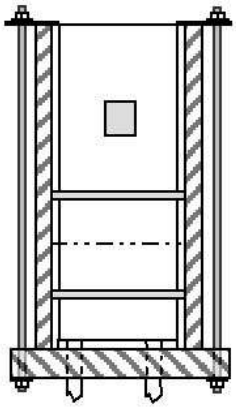

Results and Discussions

In the present analysis, simulations are carried using four different ignition sources 2.5, 3, 3.5 and 4.5 mm of ignition radius with a reaction progress variable of 0.5, initialized at the start of the simulation. The basic idea of this analysis is to verify that, which ignition radius is appropriate to choose, in order to achieve quasi-laminar phase of the premixed propagating flame. The peak overpressure and its incidence time are detailed in Table 1.

Figure 4 presents the pressure-time histories obtained from four LES simulations against experimental overpressure. Also the flame position-time histories predicted from LES simulations are compared to the experimental ones in Figure 5. Figures 6 (a) & (b) present values of the time of occurrence of peak overpressure and its magnitude, respectively, and validated against experimental measurements. It is very interesting to note from these figures, that the ignition radius of the hemi-sphere has approximately a linear relation with respect to the incidence of peak pressure. The straight horizontal line in Figure 6 (a) represents the time of experimental peak overpressure, which is roughly representing an ignition radius of about 3.5 mm. However Figure 6 (b) divulges that there is no such significant influence on the magnitude of overpressure predictions.

Snap-shots of the reaction rate contours from the LES simulations at peak overpressure time are presented in Figure 7. It reveals that irrespective of ignition radius chosen the contours are representing similar propagating flame scenario in the combustion chamber. Though Figure 7 shows very few differences, at this instance in flame position, thickness, pockets, shape of recirculation zone and structure, it is quite encouraging that all LES simulations have predicted the overall flame characteristics very well. It can also be identified that, irrespective of the radius chosen to initialize ignition, overpressure predictions show a maximum of 1-2% variation, which is quite encouraging in choosing appropriate value of ignition radius to achieve the correct timing.

Table 1. *Values of Predicted Overpressure from LES Simulations at Different Values of Ignition Radius Compared to Experimental Values*

Ignition Radius (mm)	Peak Overpressure (kPa)	Time of Incidence (msec)
2.5	54.8	5.25
3	54.8	5
3.5	54.98	4.92
4.5	53.89	4.66
Experimental	**59.9**	**4.8**

Figure 4. *Effect of Different Ignition Radii on Overpressure*

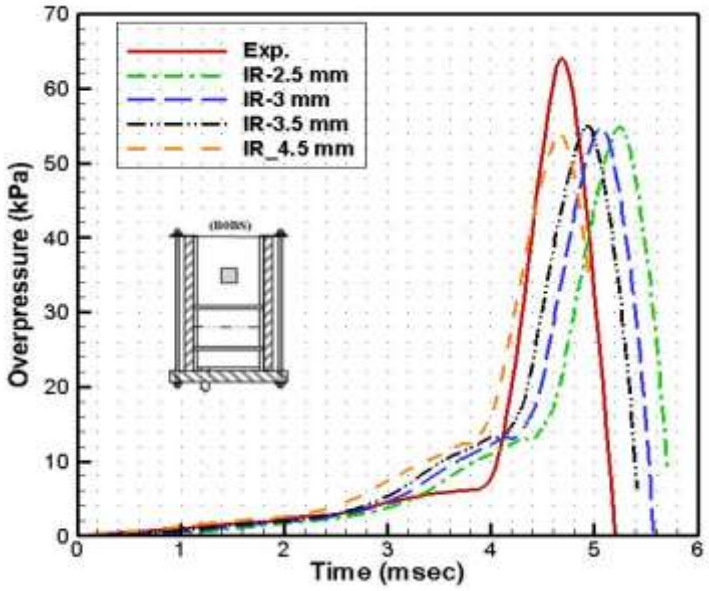

Figure 5. *Effect of Different Ignition Radii on Flame Position versus Time*

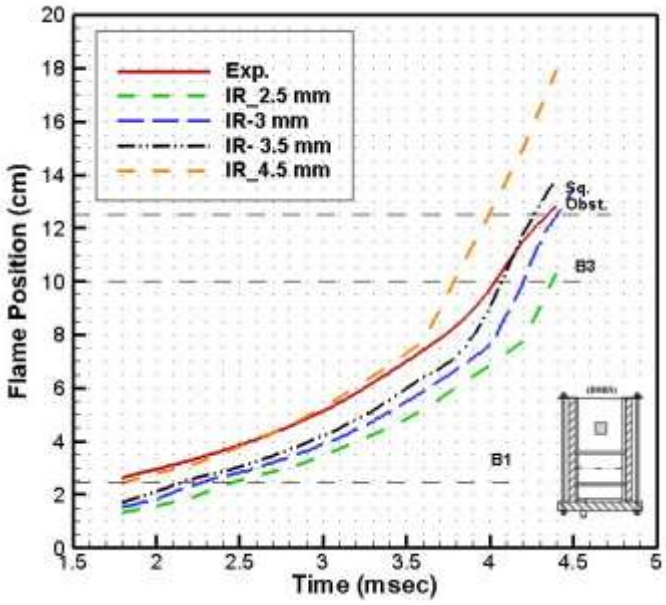

Figure 6. (a) *Time Incidence of Peak Overpressure for LES Simulations against used Ignition Radius* (b) *Values of Peak Overpressure Predicted from LES Simulations for Various Values of Ignition Radius*

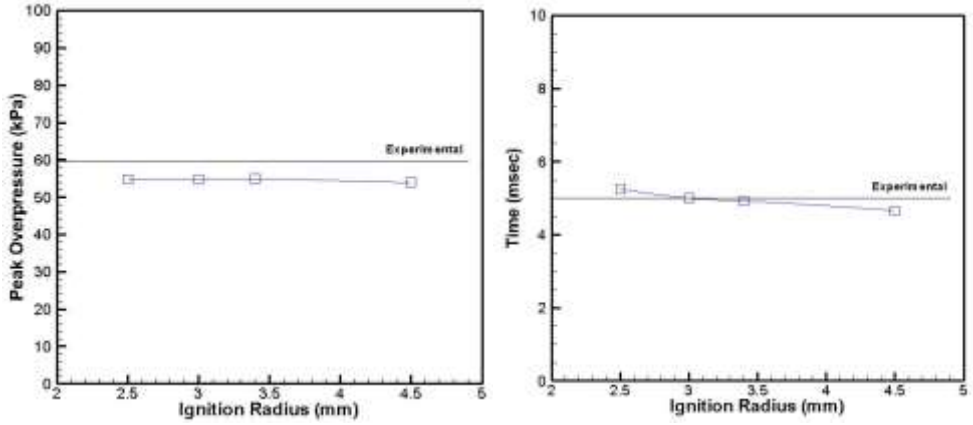

Figure 7. *Reaction Rate Contours at Peak Overpressure Incidence from LES Simulations for Ignition Radius of* (a) *2.5 mm* (b) *3 mm* (c) *3.5 mm and* (d) *4.5 mm*

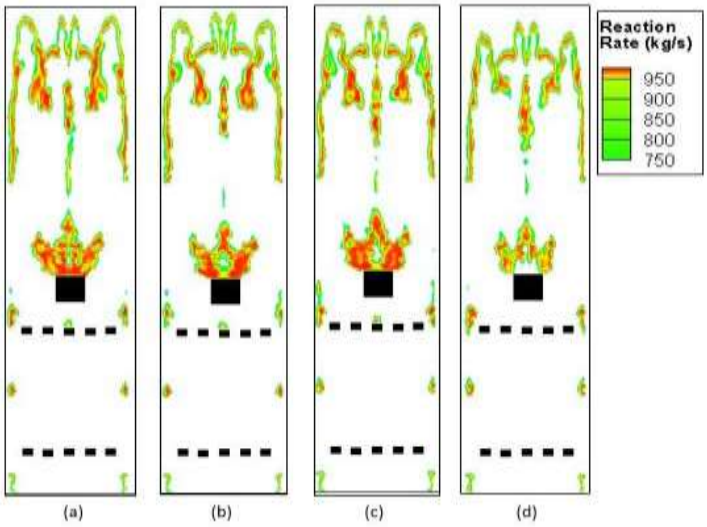

Conclusions

In the present work Large Eddy Simulation technique coupled with the dynamic flame surface density approach has been used to study the characteristics of lean burn combustion of hydrogen inside a laboratory scale premixed combustion chamber. The simulations were carried out to examine the effects of the size of ignition source on the flame structure, speed and the generated peak overpressure and its time incidence.

It was found that the ignition radius has no significant effect on the value of the predicted peak overpressure. However, it was found that there is an approximate linear relation between the size of the ignition source and the time of occurrence of the generated peak pressure.

Nomenclature

Latin Letters

C_S	Model constant used in DFSD equation
c	Reaction progress variable
D	Mass Diffusivity/ Fractal dimension
G	Convolution function or G field
h	Enthalpy, kJ/kg
L_I	Integral length scale, m
Pr	Prandtl number
Pr_t	Turbulent Prandtl number
p	Pressure, kPa
Q	Heat generation, kJ
q_c	Chemical source term, kJ/kg
R	Mean reaction rate per unit surface area, $kg/s.m^2$
S	Stress tensor, $(m/s)^2$
Sc	Schmidt number
Sc_t	Turbulent Schmidt number
S_{ij}	Strain rate, s^{-1}
T	Temperature, K
T_{ij}	Sub-test-scale stress tensor, $(m/s)^2$
t	Time, s
u	Velocity in x-direction, m/s
u'	RMS fluctuations, m/s

Greek Symbols

λ	Unresolved flame surface density, m^{-1}
μ	Dynamic viscosity, $kg/m.s$
$\bar{\mu}_{SGS}$	SGS turbulent eddy viscosity, m^2/s
$\dot{\omega}_c$	Chemical reaction rate, $^{kg/s}$
ρ	Fluid density, kg/m^3
ρ_u	Unburned gas density, kg/m^3
δ_{ij}	Kronecker delta
δ_L	Flame thickness, m
δ_c	Lower cut-off scale, m
ϕ	Any fluid property
φ	Equivalence Ratio
τ_{ij}^{sgs}	Residual stress, $(m/s)^2$
Δ	Filter width, m
Σ	Flame surface density, m^{-1}
η_k	Kolmogorov scale, m
γ	Ratio of test filter to grid filter
Λ	Unresolved flame surface density at test filter, m^{-1}

References

Abdel-Raheem M. A., Ibrahim S. S., Malalasekera W., & Masri A. R. (2013). Large Eddy Simulation of Hydrogen-Air Propagating Flames. *8th Meditrianian Combustion Symposium*, (pp. 1-8). Cesme-Izmir, Turkey.

Bray K .N. C. (1990). Studies of the Turbulent Burning Velocity. *Proceedings of the Royal Society: Mathematical and Physical Sciences, A431*(1882), 315-335.

Duwig, C., & Fuchs, L. (2007). Large Eddy Simulation of Turbulent Premixed Combustion Using A Marker Field. *Combustion Science and Technology, 179*(10), 2135-2152.

Fureby C. (2005). A fractal flame-wrinking large eddy simulation model for premixed turbulent combustion. *Proceddings of the Combustion Institute, 30*(1), 593-601.

Germano M., Piomelli U., Moin P., & Cabot W. (1991). A Dynamic Subgrid-Scale Eddy Viscosity Model. *Physics of Fluids A: Fluid Dynamics, 3*(7), 1760-1765.

Gubba S. R. (2009). *Development of a dynamic LES model for premixed turbulent flames.* Loughborough: Loughborough University.

Gubba S. R., Ibrahim S. S., Malalasekera W., & Masri A. R. (2007). An Assessment of Large Eddy Simulations of Premixed Flames Propagating past Repeated Obstacles. *Combustion Theory and Modelling, 13*(3), 513-540.

Ibrahim, S., Gubba, S., Masri, A., & Malalasekera, W. (2009). Calculations of Explosion Deflagrating Flames Using a Dynamic Flame Surface Density Model. *Journal of Loss Prevention in the Process Industries, 22*(3), 258-264.

Kent J. , Masri A. R. , & Starner S. (2005). A New Chamber to Study Premixed Flame Propagation Past Repeated Obstacles. *5th Asia-Pacific Conference on Combustion.* The University of Adelaide, Australia.

Kirkpatrick M. (2002). *A large Eddy Simulation Code for Industrial and Environmental Flows.* PhD Thesis, The University of Sydney, Australia.

Kirkpatrick, M., Armfield, S., Masri, A., & Ibrahim, S. (2003). Large eddy simulation of a propagating turbulent premixed flame. *Flow, Turbulence and Combustion*.

Knikker R., Veynante D., & Meneveau C. (2004). A dynamic flame surface density model for large eddy simulation of turbulent premixed combustion. *Phys. Fluids*(16), L91-L94.

Malalasekera, W., Ibrahim, S., Masri, A., Gubba, S., & Sadasivuni, S. (2013). Experience With the Large Eddy Simulation (LES) Technique for the Modeling of Premixed and Non-Premixed Combustion. *Heat Transfer Engineering, 34*(14).

Menon, S., & Kerstein, A. (1992). Linear-Eddy Simulation of Turbulent Premixed Flame Structure and Propagation Rate. *The American Physical, 37*(8).

Moin P., Squires K., Cabot W., & Lee S. (1991). A Dynamic Subgrid-Scale Model for Compressible Turbulence and Scalar Transport. *Physics of Fluids A: Fluid Dynamics, 3*(7), 2747-2757.

Moller S., Lundgren E., & Furbey C. (1996). Large Eddy Simulation of Unsteady Combustion. *Proceedings of the Combustion Institute, 26*(1), 241-248.

North G., & Santavicca D. (1990). The fractal nature of premixed turbulent flames. *Combustion Science and Technology, 72*(4), 215-232.

Poinot T., & Veynante D. (2005). *Theoretical and Numerical Combustion.* Philadelphia: R.T. Edwards, Inc.

Pope S.B. (1988). The Evolution of Surfaces in Turbulence. *International Journal of Engineering Science , 26*, 445-469.

Veynante D., & Poinsot T. (1997). Effects of Pressure Gradients on Turbulent Premixed Flames. *Journal of Fluid Mechanics, 353*, 83-114.

Williams F. A. (1985). Turbulent Combustion. In Buckmaster J. D. , *The Mathematics of Combustion* (pp. 97-131). Philadelphia: Society for Industrial and Applied Mathematics.